Published in IET Control Theory and Applications
Received on 2nd January 2008
Revised on 7th August 2008
doi: 10.1049/iet-cta:20080002

ISSN 1751-8644

Dynamic inversion with zero-dynamics stabilisation for quadrotor control

A. Das[1] *K. Subbarao*[2] *F. Lewis*[1]

[1]*Automation and Robotics Research Institute, The University of Texas at Arlington, 7300 Jack Newell Blvd. S., Fort Worth, TX, 76118, USA*
[2]*Department of Mechanical and Aerospace Engineering, The University of Texas at Arlington, 500 W. First Street, Arlington, TX, 76019, USA*
E-mail: adas@arri.uta.edu

Abstract: For a quadrotor, one can identify the two well-known inherent rotorcraft characteristics: underactuation and strong coupling in pitch-yaw-roll. To confront these problems and design a station-keeping and tracking controller, dynamic inversion is used. Typical applications of dynamic inversion require the selection of the output control variables to render the internal dynamics stable. This means that in many cases, perfect tracking cannot be guaranteed for the actual desired outputs. Instead, the internal dynamics of the feedback linearised system is stabilised using a robust control term. Unlike standard dynamic inversion, the linear controller gains are chosen uniquely to satisfy the tracking performance. Stability and tracking performance are guaranteed using a Lyapunov-type proof. Simulation with a typical nonlinear quadrotor dynamic model is performed to show the effectiveness of the designed control law in the presence of input disturbances.

1 Introduction

Nowadays unmanned rotorcraft are designed to operate with greater agility, and rapid manoeuvering and are capable of work in degraded environments such as wind gusts and so on. The control of these rotorcraft is a subject of research especially in applications such as rescue, surveillance, inspection, mapping and so on. For these applications, the ability of the rotorcraft to manoeuver sharply and hover precisely is important [1]. Rotorcraft control as in these applications often requires holding a particular trimmed state, generally hover, as well as making changes of velocity and acceleration in a desired way [2]. Similar to aircraft control, rotorcraft control too involves controlling the pitch, yaw and roll motion. But the main difference is that because of the unique body structure of rotorcraft (as well as the rotor dynamics and other rotating elements), the pitch, yaw and roll dynamics are strongly coupled. Therefore it is difficult to design a decoupled control law of sound structure that stabilises the faster and slower dynamics simultaneously. On the contrary, for a fixed wing aircraft it is relatively easy to design decoupled standard control laws with intuitively comprehensible structure and guaranteed performance [3]. There are many different approaches available for rotorcraft control such as [4–8] and so on. Popular methods include input–output linearisation and backstepping.

The six-degree-of-freedom airframe dynamics of a typical quadrotor involves the typical translational and rotational dynamical equations as in [2, 9]. The dynamics of a quadrotor is essentially a simplified form of helicopter dynamics that exhibits the basic problems including underactuation, strong coupling, multi-input/multi-output and unknown nonlinearities. The quadrotor is classified as a rotorcraft where lift is derived from the four rotors. Most often they are classified as helicopters as its movements are characterised by the resultant force and moments of the four rotors. Therefore the control algorithms designed for a quadrotor could be applied to a helicopter with relatively straightforward modifications. Most of the papers [5, 6, 8] and so on deal with either input–output linearisation for decoupling pitch yaw roll or backstepping to deal with the underactuation problem. The problem of coupling in the

yaw–pitch–roll of a helicopter, as well as the problem of coupled dynamics–kinematic underactuated system, can be solved by backstepping [10–12]. Dynamic inversion [3] is effective in the control of both linear and nonlinear systems and involves an inner inversion loop (similar to feedback linearisation) which results in tracking if the residual or internal dynamics is stable. Typical usage requires the selection of the output control variables so that the internal dynamics is guaranteed to be stable. This implies that the tracking control cannot always be guaranteed for the original outputs of interest.

The application of dynamic inversion on UAVs and other flying vehicles such as missiles, fighter aircrafts and so on are proposed in several research works such as [13–15] and others. It is also shown that the inclusion of dynamic neural network for estimating the dynamic inversion errors can improve the controller stability and tracking performance. Some other papers such as [16–20] and others discuss the application of dynamic inversion on nonlinear systems to tackle the model and parametric uncertainties using neural nets. It is also shown that a reconfigurable control law can be designed for fighter aircraft using neural net and dynamic inversion. Sometimes the inverse transformations required in dynamic inversion or feedback linearisation are computed by neural network to reduce the inversion error by online learning.

In this paper, we apply dynamic inversion to tackle the coupling in quadrotor dynamics which is in fact an underactuated system. Dynamic inversion is applied to the inner loop, which yields internal dynamics that are not necessarily stable. Instead of redesigning the output control variables to guarantee stability of the internal dynamics, we use a robust control approach to stabilise the internal dynamics. This yields a two-loop structured tracking controller with a dynamic inversion inner loop and an internal dynamics stabilisation outer loop. Section 2 of this paper discusses the basic quadrotor dynamics which is used for control law formulation. Section 3 shows dynamic inversion of a nonlinear state-space model of a quadrotor. Sections 4 discusses the robust control method to stabilise the internal dynamics. In Section 6, simulation results are shown to validate the control law discussed in this paper.

2 Quadrotor dynamics

Fig. 1 shows a basic model of an unmanned quadrotor. The quadrotor has some basic advantages over the conventional helicopter. Given that the front and the rear motors rotate counter-clockwise when the other two rotate clockwise, gyroscopic effects and aerodynamic torques tend to cancel in trimmed flight. This four-rotor rotorcraft does not have a swashplate [21]. In fact it does not need any blade pitch control. The collective input (or throttle input) is the sum of the thrusts of each motor (Fig. 1). Pitch movement is obtained by increasing (reducing) the speed of the rear motor and reducing (increasing) the speed of the front motor. The roll movement is obtained similarly using the lateral motors. The yaw movement is obtained by

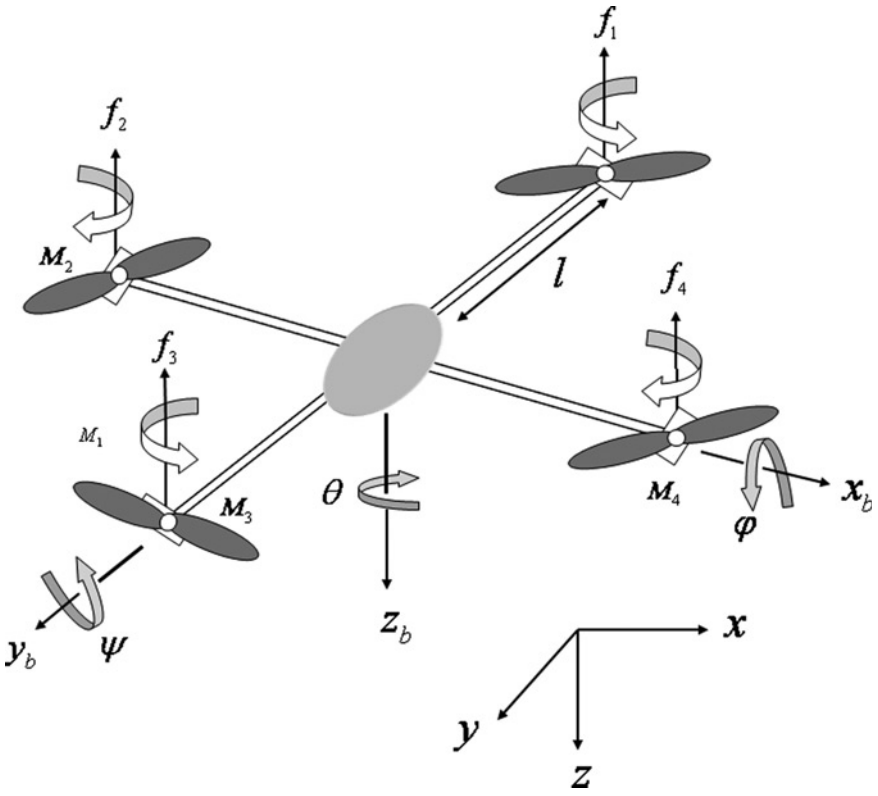

Figure 1 *Model of quadrotor Courtesy of [9, 25]*

IET Control Theory Appl., 2009, Vol. 3, Iss. 3, pp. 303–314
doi: 10.1049/iet-cta:20080002

increasing (decreasing) the speed of the front and rear motors and decreasing (increasing) the speed of the lateral motors [22].

In this section, we will describe the basic state-space model of the quadrotor. The dynamics of the four rotors are relatively much faster than the main system and thus neglected in our case. The generalised coordinates of the rotorcraft are $q = (x, y, z, \psi, \theta, \varphi)$, where (x,y,z) represents the relative position of the centre of mass of the quadrotor with respect to an inertial frame $\Im$ and (ψ, θ, φ) are the three Euler angles representing the orientation of the rotorcraft, namely yaw–pitch–roll of the vehicle.

Let us assume that the transitional and rotational coordinates are in the form $\xi = (x, y, z)^{\mathrm{T}} \in R^3$ and $\eta = (\psi, \theta, \varphi) \in R^3$. Now the total transitional kinetic energy of the rotorcraft will be $T_{\mathrm{trans}} = 1/2m\dot{\xi}^{\mathrm{T}}\dot{\xi}$, where m is the mass of the quadrotor. The rotational kinetic energy is described as $T_{\mathrm{rot}} = 1/2\dot{\eta}^{\mathrm{T}}J\dot{\eta}$, where matrix $J = J(\eta)$ is the auxiliary matrix expressed in terms of the generalised coordinates η. The potential energy in the system can be characterised by the gravitational potential, described as $U = mgz$. Defining the Lagrangian $L = T_{\mathrm{trans}} + T_{\mathrm{rot}} - U$, where $T_{\mathrm{trans}} = 1/2m\dot{\xi}^{\mathrm{T}}\dot{\xi}$ is the translational kinetic energy, $T_{\mathrm{rot}} = 1/2\omega^{\mathrm{T}}I\omega$ is the rotational kinetic energy with ω as angular speed, $U = mgz$ is the potential energy, z is the quadrotor altitude, I is the body inertia matrix and g is the acceleration due to gravity.

Then the full quadrotor dynamics is obtained as a function of the external generalised forces $F = (F_{\xi}, \tau)$ from

$$\frac{\mathrm{d}}{\mathrm{d}t}\frac{\partial L}{\partial \dot{q}} - \frac{\partial L}{\partial q} = F \tag{1}$$

The principal control inputs are defined as follows. Define

$$F_R = \begin{pmatrix} 0 \\ 0 \\ u \end{pmatrix} \tag{2}$$

where the main thrust is

$$u = f_1 + f_2 + f_3 + f_4 \tag{3}$$

and f_i's are described as $f_i = k_i\omega_i^2$, where k_i are positive constants and ω_i are the angular speed of the motor i. Then F_{ξ} can be written as

$$F_{\xi} = RF_R \tag{4}$$

where R is the transformation matrix representing the orientation of the rotorcraft as

$$R = \begin{pmatrix} c_\theta c_\psi & s_\psi s_\theta & -s_\theta \\ c_\psi s_\theta s_\varphi - s_\psi c_\varphi & s_\psi s_\theta s_\varphi + c_\psi c_\varphi & c_\theta s_\varphi \\ c_\psi s_\theta c_\varphi + s_\psi s_\varphi & s_\psi s_\theta c_\varphi - c_\psi s_\varphi & c_\theta c_\varphi \end{pmatrix} \tag{5}$$

The generalised torques for the η variables are

$$\tau = \begin{pmatrix} \tau_\psi \\ \tau_\theta \\ \tau_\varphi \end{pmatrix} \tag{6}$$

where

$$\tau_\psi = \sum_{i=1}^{4} \tau_{M_i} = c(f_1 - f_2 + f_3 - f_4) \tag{7}$$

$$\tau_\theta = (f_2 - f_4)l \tag{8}$$

$$\tau_\varphi = (f_3 - f_1)l \tag{9}$$

Thus the control distribution from the four actuator motors of the quadrotor is given by

$$\begin{pmatrix} u \\ \tau_\varphi \\ \tau_\theta \\ \tau_\psi \end{pmatrix} = \begin{pmatrix} 1 & 1 & 1 & 1 \\ -l & 0 & l & 0 \\ 0 & l & 0 & -l \\ c & -c & c & -c \end{pmatrix} \begin{pmatrix} f_1 \\ f_2 \\ f_3 \\ f_4 \end{pmatrix} \tag{10}$$

where l is the distance from the motors to the centre of gravity, τ_{M_i} is the torque produced by motor M_i and c is a constant known as force-to-moment scaling factor. So, if a required thrust and torque vector are given, one may solve for the rotor force using (10).

The final dynamic model of the quadrotor looks as

$$m\ddot{\xi} + \begin{pmatrix} 0 \\ 0 \\ mg \end{pmatrix} = F_R \tag{11}$$

$$J(\eta)\ddot{\eta} + \frac{\mathrm{d}}{\mathrm{d}t}\{J(\eta)\}\dot{\eta} - \frac{1}{2}\frac{\partial}{\partial \eta}(\dot{\eta}^{\mathrm{T}}J(\eta)\dot{\eta}) = \tau \tag{12}$$

$$J(\eta)\ddot{\eta} + \frac{\mathrm{d}}{\mathrm{d}t}\{J(\eta)\}\dot{\eta} - \bar{C}(\eta, \dot{\eta}) = \tau \tag{13}$$

$$J(\eta)\ddot{\eta} + C(\eta, \dot{\eta}) = \tau \tag{14}$$

where

$$F_R = u\begin{pmatrix} -\sin\theta \\ \cos\theta \sin\varphi \\ \cos\theta \cos\varphi \end{pmatrix}$$

and auxiliary Matrix $\{J(\eta)\} = J = T_\eta^{\mathrm{T}} I T_\eta$ with

$$T_\eta = \begin{pmatrix} -\sin\theta & 0 & 1 \\ \cos\theta \sin\psi & \cos\psi & 0 \\ \cos\theta \cos\psi & -\sin\psi & 0 \end{pmatrix}$$

Now finally the dynamic model of the quadrotor in terms of position (x, y, z) and rotation (φ, θ, ψ) is written as

$$\begin{pmatrix} \ddot{x} \\ \ddot{y} \\ \ddot{z} \end{pmatrix} = \begin{pmatrix} 0 \\ 0 \\ -g \end{pmatrix} + \frac{1}{m} \begin{pmatrix} -\sin\ \theta \\ \cos\ \theta\ \sin\ \varphi \\ \cos\ \theta\ \cos\ \varphi \end{pmatrix} u \tag{15}$$

$$\begin{pmatrix} \ddot{\varphi} \\ \ddot{\theta} \\ \ddot{\psi} \end{pmatrix} = f(\varphi, \theta, \psi) + g(\varphi, \theta, \psi)\tau \tag{16}$$

where

$$f(\varphi, \theta, \psi) = \begin{pmatrix} \dot{\theta}\dot{\psi}\left(\frac{I_y - I_z}{I_x}\right) - \frac{J_p}{I_x}\dot{\theta}\Omega \\ \dot{\varphi}\dot{\psi}\left(\frac{I_z - I_x}{I_y}\right) + \frac{J_p}{I_y}\dot{\varphi}\Omega \\ \dot{\varphi}\dot{\theta}\left(\frac{I_x - I_y}{I_z}\right) \end{pmatrix},$$

$$g(\varphi, \theta, \psi) = \begin{pmatrix} \frac{l}{I_x} & 0 & 0 \\ 0 & \frac{l}{I_y} & 0 \\ 0 & 0 & \frac{l}{I_z} \end{pmatrix}, \quad u \in R^1 \quad \text{and}$$

$$\tau = \begin{bmatrix} \tau_\varphi \\ \tau_\theta \\ \tau_\psi \end{bmatrix} \in R^3$$

are the control inputs, $I_{x,y,z}$ are body inertia, J_p is propeller/rotor inertia and $\Omega = \omega_2 + \omega_4 - \omega_1 - \omega_3$. Thus the system is the form of an underactuated system with six outputs and four inputs.

3 Dynamic inversion inner control loop

Dynamic inversion [3] is an approach where a feedback linearisation loop is applied to the tracking outputs of interest. The residual dynamics, not directly controlled, is known as the internal dynamics. If the internal dynamics are stable, dynamic inversion is successful. Typical usage requires the selection of the output control variables so that the internal dynamics is guaranteed to be stable. This means that tracking cannot always be guaranteed for the original outputs of interest.

In this paper, we apply dynamic inversion to the system given by (15) and (16) to achieve station-keeping tracking control for the position outputs (x, y, z, ψ). Initially we select the convenient output vector $y_1 = (z, \varphi, \theta, \psi)$ that makes the dynamic inverse easy to find. Dynamic inversion now yields effectively an inner control loop that feedback linearises the system from the control $u_b = (u, \tau_\varphi, \tau_\theta, \tau_\psi)$ to the output $y_1 = (z, \varphi, \theta, \psi)$.

Note, however, that y_1 is not the desired system output. Moreover, dynamic inversion generates a specific internal dynamics, as detailed below, which may not always be stable. Therefore a second outer loop is designed to generate the required values for $y_1 = (z, \varphi, \theta, \psi)$ in terms of the values of the desired tracking output (x, y, z, ψ). A robustifying term is then added to stabilise the internal dynamics. An overall Lyapunov proof guarantees stability and performance. The following background is required. Consider a nonlinear system of the form

$$\dot{q} = f(q, u_q) \tag{17}$$

where $u_q \in R^m$ is the control input and $q \in R^n$ is the state vector. The technique of designing the control input u using dynamic inversion involves two steps. First, one finds a state transformation $z = z(q)$ and an input transformation $u_q = u_q(q, v)$ so that the nonlinear system dynamics is transformed into an equivalent linear time-invariant dynamics of the form

$$\dot{z} = az + bv \tag{18}$$

where $a \in R^{n \times n}$ and $b \in R^{n \times m}$ are constant matrices with v is known as new input to the linear system. Secondly, one can design v easily from the linear control theory approach such as pole placement and so on. To obtain the desired linear equations (18), one has to differentiate outputs until input vector u appears. That is, for a set of output $y = h(q)$ with $h \in R^m$ if

$$y^r = M(q) + E(q)u_q \tag{19}$$

then the desired input which cancels the nonlinearities in the system is obtained as

$$u_q = E(q)^{-1}(-M(q) + v) \tag{20}$$

where $E(q) \in R^{m \times m}$ and $M(q) \in R^{m \times 1}$. This control is known as dynamic inverse. r is known as the relative degree of the system and generally $r < n$; if $r = n$ then full state feedback linearisation is achieved if $E(q)$ is invertible. Note that for multi-input multi-output system, if number of outputs is not equal to the number of inputs (underactuated system), then $E(q)$ becomes non-square and is difficult to obtain a feasible linearising input u_q.

Systems (15) and (16) are an underactuated system if we consider the states $(x, y, z, \varphi, \theta, \psi)$ as outputs and $u_b = (u, \tau_\varphi, \tau_\theta, \tau_\psi)$ as inputs. To overcome these difficulties, we consider four outputs $y_1 = (z, \varphi, \theta, \psi)$ which are used for feedback linearisation. Differentiating the output vector twice with respect to the time, we obtain

doi: 10.1049/iet-cta:20080002

from (15) and (16) that

$$\ddot{y}_1 = \begin{bmatrix} \ddot{z} \\ \ddot{\varphi} \\ \ddot{\theta} \\ \ddot{\psi} \end{bmatrix} = M_b + E_b u_b \tag{21}$$

where

$$M_b = \begin{bmatrix} -g \\ \dot{\theta}\dot{\psi}\left(\frac{I_y - I_z}{I_x}\right) - \frac{J_p}{I_x}\dot{\theta}\Omega \\ \dot{\varphi}\dot{\psi}\left(\frac{I_z - I_x}{I_y}\right) + \frac{J_p}{I_y}\dot{\varphi}\Omega \\ \dot{\varphi}\dot{\theta}\left(\frac{I_x - I_y}{I_z}\right) \end{bmatrix},$$

$$E_b = \begin{bmatrix} -\left(\frac{1}{\mathrm{m}}\right)\cos\theta\cos\varphi & 0 & 0 & 0 \\ 0 & \frac{l}{I_x} & 0 & 0 \\ 0 & 0 & \frac{l}{I_y} & 0 \\ 0 & 0 & 0 & \frac{l}{I_z} \end{bmatrix} \quad \text{and}$$

$$u_b = \begin{bmatrix} u \\ \tau_\varphi \\ \tau_\theta \\ \tau_\psi \end{bmatrix}$$

It is seen that for invertibility of E_b, $0 \leq \theta, \varphi < 90^\circ$. Equation (21) is equivalent to (19); the relative degree of the system is calculated as 8, whereas the order of the system is 12. So, the remaining dynamics which does not come out in the process of feedback linearisation is known as internal dynamics. To guarantee the stability of the whole system, it is mandatory to guarantee the stability of the remaining fourth-order dynamics. In the next section, we will discuss how to control the internal dynamics using a backstepping approach. Now using (20), we can write the desired input to the system

$$u_b = E_b^{-1}(-M_b + v_b) \tag{22}$$

which yields

$$\ddot{y}_1 = v_b \tag{23}$$

where $v_b = \begin{pmatrix} v_z & v_\varphi & v_\theta & v_\psi \end{pmatrix}^{\mathrm{T}}$. This system is decoupled and linear. The auxiliary input v_b is designed as described below.

3.1 FBLC linear controller

Assuming the desired output to the system is $y_{\mathrm{d}} = \begin{pmatrix} z_{\mathrm{d}} & \varphi_{\mathrm{d}} & \theta_{\mathrm{d}} & \psi_{\mathrm{d}} \end{pmatrix}^{\mathrm{T}}$, the linear controller v_b is designed as

$$v_b = \begin{bmatrix} v_z \\ v_\varphi \\ v_\theta \\ v_\psi \end{bmatrix} = \begin{bmatrix} \ddot{z}_{\mathrm{d}} - K_{1_z}(\dot{z} - \dot{z}_{\mathrm{d}}) - K_{2_z}(z - z_{\mathrm{d}}) \\ \ddot{\varphi}_{\mathrm{d}} - K_{1_\varphi}(\dot{\varphi} - \dot{\varphi}_{\mathrm{d}}) - K_{2_\varphi}(\varphi - \varphi_{\mathrm{d}}) + v_{r_\varphi} \\ \ddot{\theta}_{\mathrm{d}} - K_{1_\theta}(\dot{\theta} - \dot{\theta}_{\mathrm{d}}) - K_{2_\theta}(\theta - \theta_{\mathrm{d}}) + v_{r_\theta} \\ \ddot{\psi}_{\mathrm{d}} - K_{1_\psi}(\dot{\psi} - \dot{\psi}_{\mathrm{d}}) - K_{2_\psi}(\psi - \psi_{\mathrm{d}}) \end{bmatrix} \tag{24}$$

where $K_{1_\varphi}, K_{2_\varphi}, \ldots,$ and so on are positive constants so that the poles of the error dynamics arising from (23) and (24) are in the left half of the s-plane. For hovering control, z_{d} and ψ_{d} are chosen depending on the designer choice. We note that, v_{r_φ} and v_{r_θ} are the robustifying terms. Now, the other reference inputs such as $(\varphi_{\mathrm{d}}, \theta_{\mathrm{d}})$ are derived such that the internal dynamics are rendered stable as shown below. Let us define the state error $e_1 = (z_{\mathrm{d}} - z \quad \varphi_{\mathrm{d}} - \varphi \quad \theta_{\mathrm{d}} - \theta \, \psi_{\mathrm{d}} - \psi)^{\mathrm{T}}$ and a sliding error as

$$r_1 = \dot{e}_1 + \Lambda_1 e_1 \tag{25}$$

where Λ_1 is a diagonal positive-definite design parameter matrix. Common usage is to select Λ_1 diagonal with positive entries. Then, (25) is a stable system so that e_1 is bounded as long as the controller guarantees that the filtered error r_1 is bounded. In fact it is easy to show [23] that one has

$$\|e_1\| \leq \frac{\|r_1\|}{\sigma_{\min}(\Lambda_1)}, \quad \|\dot{e}_1\| \leq \|r_1\| \tag{26}$$

Note that $\dot{e}_1 + \Lambda_1 e_1 = 0$ defines a stable sliding mode surface. The function of the controller to be designed is to force the system onto this surface by making r_1 small. The parameter Λ_1 is selected for a desired sliding mode response

$$e_1(t) = e_1^{-\Lambda_1 t} e_1(0) \tag{27}$$

We now focus on designing a controller to keep $\|r_1\|$ small. From (25),

$$\dot{r}_1 = \ddot{e}_1 + \Lambda_1 \dot{e}_1 \tag{28}$$

Adding an integrator to the linear controller given in (24), and now we can rewrite (24) as

$$v_b = \ddot{y}_{b_{\mathrm{d}}} + K_1 \dot{e}_1 + K_2 e_1 + K_3 \int_0^t r_1 \, \mathrm{d}t + V_r \tag{29}$$

where $y_{b_{\mathrm{d}}} = \left[\ddot{z}_{\mathrm{d}}, \ddot{\varphi}_{\mathrm{d}}, \ddot{\theta}_{\mathrm{d}}, \ddot{\psi}_{\mathrm{d}}\right]^{\mathrm{T}}$, $K_i = \mathrm{diag}(K_{i_z}, K_{i_\varphi}, K_{i_\theta}, K_{i_\psi}) > 0$, $i = 1, 2, 3, 4$ and $V_r = \left[0, v_{r_\varphi}, v_{r_\theta}, 0\right]^{\mathrm{T}}$.

Now using (22) and (29), we can rewrite (21) in the form of error dynamics as

$$\ddot{e}_1 + K_1\dot{e}_1 + K_2 e_1 + K_3\int_0^t r_1\,\mathrm{d}t + V_r = 0 \tag{30}$$

Thus (28) becomes

$$\dot{r}_1 = -K_1\dot{e}_1 - K_2 e_1 - K_3\int_0^t r_1\,\mathrm{d}t + \Lambda_1\dot{e}_1 - V_r \tag{31}$$

If we choose $K_1 = (\Lambda_1 + R)$ and $K_2 = \Lambda_1 R$, then equation (31) will be look like

$$\dot{r}_1 = -Rr_1 - K_3\int_0^t r_1\,\mathrm{d}t - V_r \tag{32}$$

4 Desired tracking loop and stabilization of the internal dynamics

The internal dynamics [12] for the feedback linearised system are given by

$$\ddot{x} = -\frac{u}{m}\sin\theta \tag{33}$$

$$\ddot{y} = \frac{u}{m}\cos\theta\sin\varphi \tag{34}$$

For the stability of the whole system as well as for the tracking purposes, x and y should be bounded and controlled in a desired way. Note that the height z is controlled by the linear controller (24).

To stabilise the zero dynamics, we select some desired θ_d and φ_d such that (x, y) is bounded. Then that $(\theta_\mathrm{d}, \varphi_\mathrm{d})$ is given to (24) as a reference. Therefore let us redefine (33) as

$$\ddot{x} = -\frac{u}{m}\theta_\mathrm{d} - \frac{u}{m}(-\tilde{\theta}) \tag{35}$$

$$\ddot{y} = \frac{u}{m}\varphi_\mathrm{d} - \frac{u}{m}\tilde{\varphi} \tag{36}$$

where,

$$\theta_\mathrm{d} = -\frac{m}{u}\left\{\ddot{x}_\mathrm{d} + C_{11}(\dot{x}_\mathrm{d} - \dot{x}) + C_{12}(x_\mathrm{d} - x) + C_{13}\right\} \tag{37}$$

$$\varphi_\mathrm{d} = \frac{m}{u}\left\{\ddot{y}_\mathrm{d} + C_{21}(\dot{y}_\mathrm{d} - \dot{y}) + C_{22}(y_\mathrm{d} - y)\right\} \tag{38}$$

$$\tilde{\theta} = \theta_\mathrm{d} - \sin\theta \tag{39}$$

$$\tilde{\varphi} = \varphi_\mathrm{d} - \cos\theta\,\sin\varphi \tag{40}$$

and

$$\tilde{A} = \begin{bmatrix} -\tilde{\theta} \\ \tilde{\varphi} \end{bmatrix} \tag{41}$$

with $C_{ij} > 0,\ i, j = 1, 2$.

Define the state error

$$e_2 = \begin{pmatrix} x_\mathrm{d} - x & y_\mathrm{d} - y \end{pmatrix}^\mathrm{T} \tag{42}$$

and the sliding mode error for the internal dynamics as

$$r_2 = \dot{e}_2 + \Lambda_2 e_2 \tag{43}$$

where Λ_2 is a diagonal positive-definite design parameter matrix with similar characteristic of Λ_1. Then designing a controller to keep $\|r_2\|$ small will guarantee that $\|e_2\|$ and $\|\dot{e}_2\|$ are small. Differentiating r_2 we obtain

$$\dot{r}_2 = \ddot{e}_2 + \Lambda_2\dot{e}_2 \tag{44}$$

Combining (35)–(44), we obtain

$$\ddot{e}_2 + C_1\dot{e}_2 + C_2 e_2 - U_m\tilde{A} + C_3\int_0^t r_2\,\mathrm{d}t = 0 \tag{45}$$

where $U_m = u/m$. Therefore

$$\dot{r}_2 = -C_1\dot{e}_2 - C_2 e_2 - C_3\int_0^t r_2\,\mathrm{d}t + U_m\tilde{A} + \Lambda_2\dot{e}_2 \tag{46}$$

Let

$$C_1 = \Lambda_2 + S_0 \tag{47}$$

$$C_2 = \Lambda_2 S_0 \tag{48}$$

Therefore

$$\dot{r}_2 = -(\Lambda_2 + S_0)\dot{e}_2 - \Lambda_2 S_0 e_2 - C_3\int_0^t r_2\,\mathrm{d}t + U_m\tilde{A} + \Lambda_2\dot{e}_2 \tag{49}$$

$$\dot{r}_2 = -S_0 r_2 - C_3\int_0^t r_2\,\mathrm{d}t + U_m\tilde{A} \tag{50}$$

5 Controller structure and stability analysis

The overall control system has two loops and is depicted in Fig. 2. The following theorem details the performance of the controller.

Definition 1: The equilibrium point x_e is said to be uniformly ultimately bounded (UUB) if there exist a compact set $S \subset R^n$ so that for all $x_0 \in S$ there exist a bound B and a time $T(B, x_0)$ such that $\|x(t) - x_e(t)\| \le B\ \forall t \ge t_0 + T$.

Theorem 1: Given the system as described in (15) and (16) with a control law shown in Fig. 2 and given by (22), (29), (37), (38). The robustifying term is $V_\mathrm{r} = \left[0, v_{r_\varphi}, v_{r_\theta}, 0\right]^\mathrm{T} = P_s^\mathrm{T} r_1\left(r_1^\mathrm{T} P_s P_s^\mathrm{T} r_1\right)^{-1} r_2^\mathrm{T} Q_1 U_m\tilde{A}$ with P_s and Q_1 defined in

doi: 10.1049/iet-cta:20080002

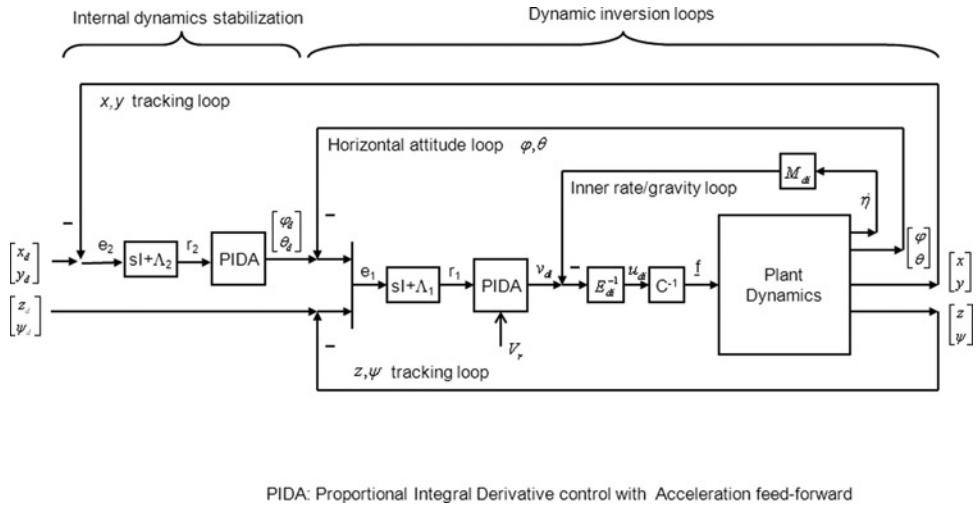

Figure 2 *Control block diagram*

the proof and $U_m = u/m$. Then, the tracking errors r_1 and r_2 and thereby e_1 and e_2 are UUB with practical bounds (59), (61) and can be made arbitrarily small with a suitable choice of gain parameters. According to the definition given by (25) of r_1 and (43) of r_2, this guarantees that e_1 and e_2 are UUB because

$$\begin{aligned} \|e_1\| &\le \frac{\|r_1\|}{\sigma_{\min}(\Lambda_1)} \le \frac{b_{r_1}}{\sigma_{\min}(\Lambda_1)} \quad b_{r_1} > 0 \\ \|e_2\| &\le \frac{\|r_2\|}{\sigma_{\min}(\Lambda_2)} \le \frac{b_{r_2}}{\sigma_{\min}(\Lambda_2)} \quad b_{r_2} > 0 \end{aligned} \tag{51}$$

where $\sigma_{\min}(\Lambda_i)$ is the minimum eigenvalue of Λ_i $i = 1, 2$.

Proof: Consider the Lyapunov function

$$\begin{aligned} L = {} & \frac{1}{2} r_1^{\mathrm{T}} P_1 r_1 + \frac{1}{2} r_2^{\mathrm{T}} Q_1 r_2 + \frac{1}{2}\left[\int_0^t r_1^{\mathrm{T}}\,\mathrm{d}t\right] P_2 \left[\int_0^t r_1\,\mathrm{d}t\right] \\ & + \frac{1}{2}\left[\int_0^t r_2^{\mathrm{T}}\,\mathrm{d}t\right] Q_2 \left[\int_0^t r_2\,\mathrm{d}t\right] \end{aligned} \tag{52}$$

with symmetric matrices P_1, P_2, Q_1, $Q_2 > 0$.

Therefore by differentiating L we will obtain

$$\begin{aligned} \dot{L} = {} & -r_1^{\mathrm{T}} P_1 R r_1 - r_1^{\mathrm{T}} P_1 K_3 \int_0^t r_1\,\mathrm{d}t + r_1 P_2 \int_0^t r_1\,\mathrm{d}t - r_2^{\mathrm{T}} Q_1 S_0 r_2 \\ & - r_2^{\mathrm{T}} Q_1 C_3 \int_0^t r_2\,\mathrm{d}t + r_2^{\mathrm{T}} Q_2 \int_0^t r_2\,\mathrm{d}t + r_2^{\mathrm{T}} Q_1 U_m \tilde{A} - r_1^{\mathrm{T}} P_1 V_r \end{aligned} \tag{53}$$

If $P_2 = P_1 K_3$ and $Q_2 = Q_1 C_3$, then integration term vanishes.

$$\dot{L} = -r_1^{\mathrm{T}} P_1 R r_1 - r_2^{\mathrm{T}} Q_1 S_0 r_2 + r_2^{\mathrm{T}} Q_1 U_m \tilde{A} - r_1^{\mathrm{T}} P_1 V_r \tag{54}$$

Let us define that q_{ij} and p_{ij} denote the element of the matrices Q_1 and P_1, respectively. Now it is possible to find appropriate v_{r_φ} and v_{r_θ} to construct a suitable V_r for cancelling the term $r_2^{\mathrm{T}} Q_1 U_m \tilde{A}$.

Define, $P_s = \begin{bmatrix} 0 & p_{22} & 0 & 0 \\ 0 & 0 & p_{33} & 0 \end{bmatrix}^{\mathrm{T}}$ and $V_r = \left[0, v_{r_\varphi}, v_{r_\theta}, 0\right]^{\mathrm{T}} = P_s^{\mathrm{T}} r_1 \left(r_1^{\mathrm{T}} P_s P_s^{\mathrm{T}} r_1\right)^{-1} r_2^{\mathrm{T}} Q_1 U_m \tilde{A}$, then the following cases will arise: assume that ε is a very small positive number near zero.

Case 1: When $\left\| r_1^{\mathrm{T}} P_s P_s^{\mathrm{T}} r_1 \right\| > \varepsilon$ then

$$\dot{L} = -r_1^{\mathrm{T}} P_1 R r_1 - r_2^{\mathrm{T}} Q_1 S_0 r_2 \le 0 \tag{55}$$

Case 2: When $\left\| r_1^{\mathrm{T}} P_s P_s^{\mathrm{T}} r_1 \right\| \le \varepsilon$ then

$$\dot{L} = -r_1^{\mathrm{T}} P_1 R r_1 - r_2^{\mathrm{T}} Q_1 S_0 r_2 - \left(\frac{r_1^{\mathrm{T}} P_s P_s^{\mathrm{T}} r_1}{\varepsilon} - 1\right) r_2^{\mathrm{T}} Q_1 U_m \tilde{A} \tag{56}$$

or

$$\begin{aligned} \dot{L} \le {} & -\|r_1\|^2 P_{R_{\min}} - \|r_2\|^2 Q_{S_{\min}} - \frac{\|r_1\|^2 \|r_2\| A_{PQ_{\min}}}{\varepsilon} \\ & + \|r_2\| A_{QU_{\max}} \end{aligned} \tag{57}$$

where $P_{R_{\min}}$, $Q_{S_{\min}}$, $A_{PQ_{\min}}$ are the minimum singular values of $P_1 R$, $Q_1 S_0$ and $P_S P_S^{\mathrm{T}} Q_1 U_m \tilde{A}$, respectively. Similarly, $A_{QU_{\max}}$ is the maximum singular value of $Q_1 U_m \tilde{A}$ and

$$\begin{aligned} \dot{L} \le {} & -\|r_1\|^2 P_{R_{\min}} - \|r_2\|^2 Q_{S_{\min}} \\ & - \|r_2\| \left(\frac{\|r_1\|^2 A_{PQ_{\min}}}{\varepsilon} - A_{QU_{\max}}\right) \end{aligned} \tag{58}$$

So, $\dot{L} \leq 0$ as long as

$$\|r_1\| > \sqrt{\frac{\varepsilon A_{QU_{\max}}}{A_{PQ_{\min}}}} = b_{r_1} \tag{59}$$

Again from (57), we can rewrite

$$\dot{L} \leq -\|r_1\|^2 P_{R_{\min}} - \frac{\|r_1\|^2 \|r_2\| A_{PQ_{\min}}}{\varepsilon} - \|r_2\|\left(\|r_2\| Q_{S_{\min}} - A_{QU_{\max}}\right) \tag{60}$$

So, $\dot{L} \leq 0$ as long as

$$\|r_2\| > \frac{A_{QU_{\max}}}{Q_{S_{\min}}} = b_{r_2} \tag{61}$$

Thus, $\dot{L}$ is negative outside a compact set. Selecting the gains P_1, R, Q_1, S_0 ensures that the compact set defined by $\|r_1\| \leq b_{r_1}$ and $\|r_2\| \leq b_{r_2}$ is bounded. This ensures UUB for r_1 and r_2 stated in (59) and (61), respectively. Also, from (26), it trivially follows that $\|e_1\| \leq (\sigma_{\min}(\Lambda_1))^{-1} b_{r_1}$ and $\|e_2\| \leq (\sigma_{\min}(\Lambda_2))^{-1} b_{r_2}$. □

6 Simulation results

6.1 Rotorcraft parameters

Simulation for a typical quadrotor is performed using the parameters (SI unit)

$$M_1 = \begin{bmatrix} 1\text{ kg} & 0 & 0 \\ 0 & 1\text{ kg} & 0 \\ 0 & 0 & 1\text{ kg} \end{bmatrix},$$

$$I = \begin{bmatrix} 5\text{ kg m}^2 & 0 & 0 \\ 0 & 5\text{ kg m}^2 & 0 \\ 0 & 0 & 15\text{ kg m}^2 \end{bmatrix}, \quad J_p = 2\text{kg m}^2$$

$$g = 9.81\text{ m/s}^2$$

6.2 Reference trajectory generation

As outlined in [24, 25], a reference trajectory is derived that minimises the jerk (rate of change of acceleration) over the time horizon. The trajectory ensures that the velocities and accelerations at the end point are zero while meeting the position tracking objective. The following summarises this approach:

$$\dot{x}_{\mathrm{d}}(t) = a_{1_x} + 2a_{2_x}t + 3a_{3_x}t^2 + 4a_{4_x}t^3 + 5a_{5_x}t^4 \tag{62}$$

Differentiating again

$$\ddot{x}_{\mathrm{d}}(t) = 2a_{2_x} + 6a_{3_x}t + 12a_{4_x}t^2 + 20a_{5_x}t^3 \tag{63}$$

As we indicated before that initial and final velocities and accelerations are zero; so from (62) we can conclude

$$\begin{bmatrix} d_x \\ 0 \\ 0 \end{bmatrix} = \begin{bmatrix} 1 & t_{\mathrm{f}} & t_{\mathrm{f}}^2 \\ 3 & 4t_{\mathrm{f}} & 5t_{\mathrm{f}}^2 \\ 6 & 12t_{\mathrm{f}} & 20t_{\mathrm{f}}^2 \end{bmatrix} \begin{bmatrix} a_{3_x} \\ a_{4_x} \\ a_{5_x} \end{bmatrix} \tag{64}$$

where $d_x = \left(x_{d_{\mathrm{f}}} - x_{d_0}\right)/t_{\mathrm{f}}^3$. Now, solving for coefficients

$$\begin{bmatrix} a_{3_x} \\ a_{4_x} \\ a_{5_x} \end{bmatrix} = \begin{bmatrix} 1 & t_{\mathrm{f}} & t_{\mathrm{f}}^2 \\ 3 & 4t_{\mathrm{f}} & 5t_{\mathrm{f}}^2 \\ 6 & 12t_{\mathrm{f}} & 20t_{\mathrm{f}}^2 \end{bmatrix}^{-1} \begin{bmatrix} d_x \\ 0 \\ 0 \end{bmatrix} \tag{65}$$

Thus the desired trajectory for the x-direction is given by

$$x_{\mathrm{d}}(t) = x_{d_0} + a_{3_x}t^3 + a_{4_x}t^4 + a_{5_x}t^5 \tag{66}$$

Similarly, the reference trajectories for the y and z directions are given by (67) and (68), respectively, as

$$y_{\mathrm{d}}(t) = y_{\mathrm{d}_0} + a_{3_y}t^3 + a_{4_y}t^4 + a_{5_y}t^5 \tag{67}$$

$$z_{\mathrm{d}}(t) = z_{\mathrm{d}_0} + a_{3_z}t^3 + a_{4_z}t^4 + a_{5_z}t^5 \tag{68}$$

The advantage of this trajectory generation method lies in the fact that more demanding changes in position can be accommodated by varying the final time, that is, acceleration/torque ratio can be controlled smoothly as per requirement and constraints explicitly enforced on the achievable accelerations. For example, let us assume at $t = 0$, $x_{\mathrm{d}_0} = 0$ and at $t = 10\,\mathrm{s}$, $x_{d_f} = 10$. Therefore $d_x = 0.01$ and the trajectory is given by (69) and is as shown in Fig. 3 for various desired final positions.

$$x_{\mathrm{d}}(t) = 0.1t^3 - 0.015t^4 + 0.0006t^5 \tag{69}$$

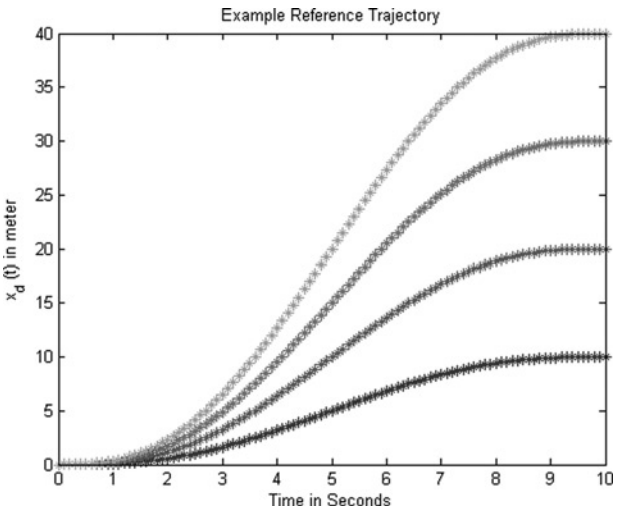

Figure 3 *Example trajectory simulation for different final positions*

IET Control Theory Appl., 2009, Vol. 3, Iss. 3, pp. 303–314
doi: 10.1049/iet-cta:20080002

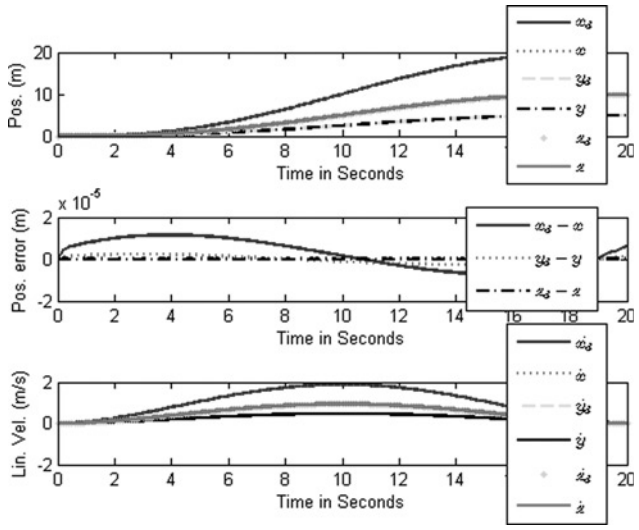

Figure 4 *Position tracking – simultaneous command in x, y and z*

6.3 Simulation result without disturbances

6.3.1 Case-1: From initial position at (0, 0, 0) to final position at (20, 5, 10): Fig. 4 describes the controlled motion of the quadrotor from its initial position (0, 0, 0) to final position (20, 5, 10) for a given time (20 s). The actual trajectories $x(t)$, $y(t)$ and $z(t)$ match exactly their desired values $x_d(t)$, $y_d(t)$ and $z_d(t)$, respectively, nearly exactly. The errors along the three axes are also shown in the same figure. It can be seen that the tracking is almost perfect as well as the tracking errors are significantly small. Linear velocities of the quadrotor are also shown in the same figure also. Fig. 5 describes the attitude of the quadrotor φ, θ along with their demands φ_d, θ_d and attitude errors in radian. Again the angles match their command values nearly perfectly. Angular velocities are also shown in the same figure. Fig. 6 describes the control input requirement which is very much realisable. Note that as described before the control requirement for yaw angle is $\tau_\psi = 0$ and it is seen from Fig. 6.

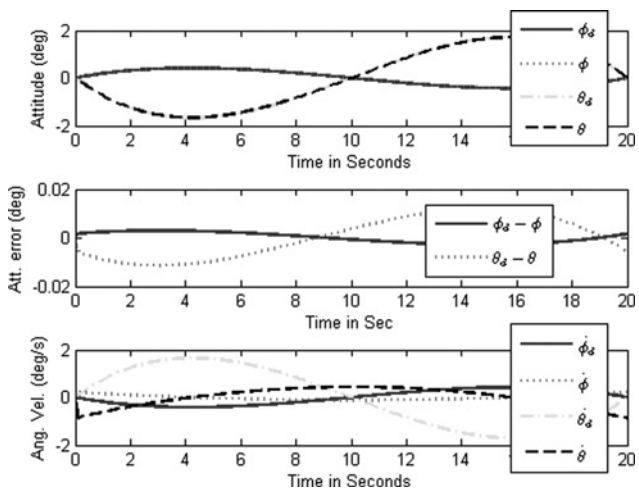

Figure 5 *Resultant angular positions, errors and velocities*

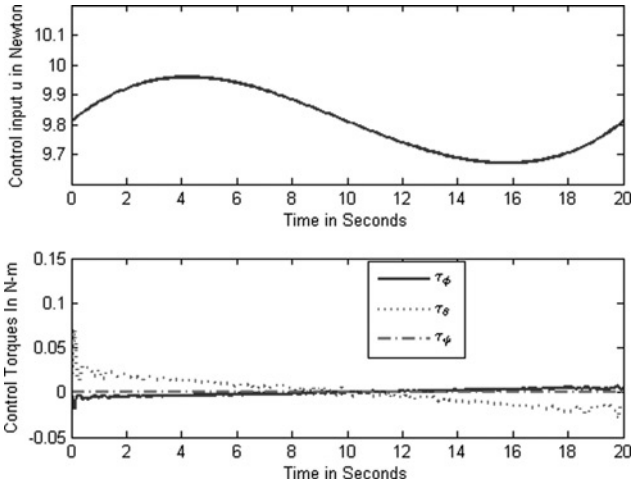

Figure 6 *Input commands for Case 1*

6.3.2 Case-2: From initial position at (0, 5, 10) to final position at (20, 5, 10): Figs. 7 and 8 illustrate the decoupling phenomenon of the control law. Fig. 7 shows that $x(t)$ follows the command $x_d(t)$ nearly perfect, whereas $y(t)$ and $z(t)$ are held their initial values. Fig. 8 shows that the change in x does not make any influence on φ. The corresponding control inputs are also shown in Fig. 9 and due to the full decoupling effect it is seen that τ_φ is almost zero.

The similar type of simulations are performed for y- and z-directional motions separately and similar plots are obtained showing excellent tracking.

6.4 Simulation with unmodelled input disturbances

The simulation is performed to verify its robustness properties against unmodelled input disturbances. For this

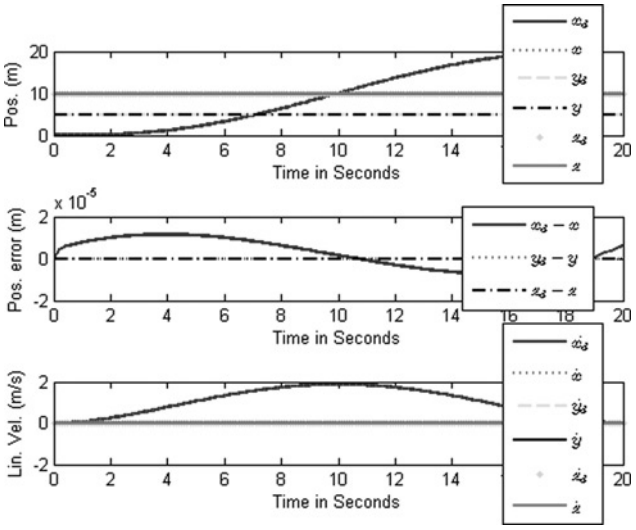

Figure 7 *Position tracking (x command only)*

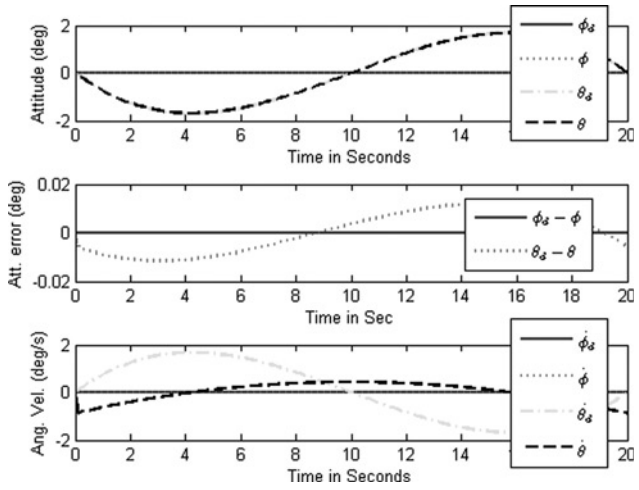

Figure 8 *Angular variations and rates (x command tracking)*

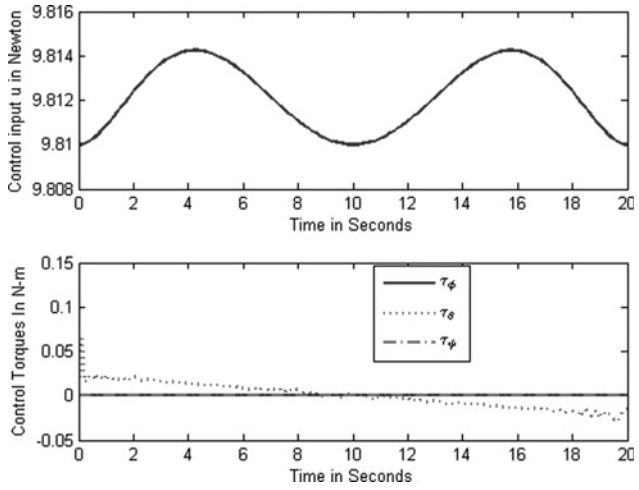

Figure 9 *Input commands for x-command tracking (Case 2)*

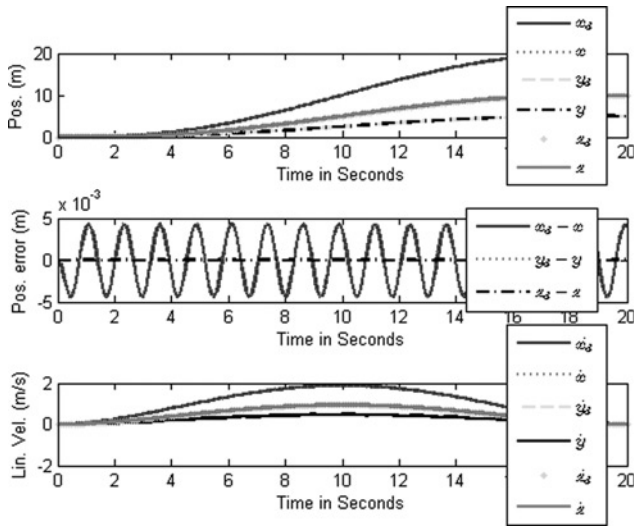

Figure 10 *Position tracking – simultaneous command in x, y and z + input disturbances*

case, we simulate the dynamics with high-frequency disturbance $\sin(5t)$ (10% of maximum magnitude of force) for force channel and $0.01\sin(5t)$ (~15% of maximum angular acceleration) for torque channel.

6.4.1 Case-3: From initial position at (0, 0, 0) to final position at (20, 5, 10): Figs. 10 and 11 describe the motion of the quadrotor from its initial position (0, 0, 0) to final position (20, 5, 10) for a given time (20 s) with input disturbances. It can be seen from Fig. 10 that the quadrotor can track the desired position effectively without any effect of high input disturbances. From Figs. 10 and 11, it is also seen that the position errors are bounded and small. Fig. 12 shows the bounded variation of control inputs in the presence of disturbance. Similar tracking performance is obtained for other commanded motion.

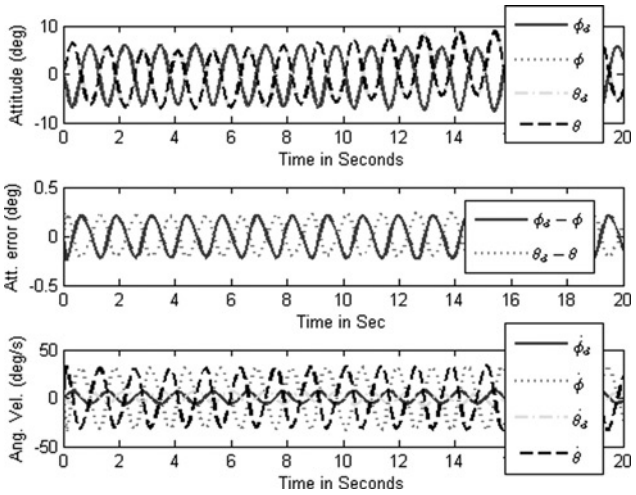

Figure 11 *Angular variations, errors and velocities (with input disturbances)*

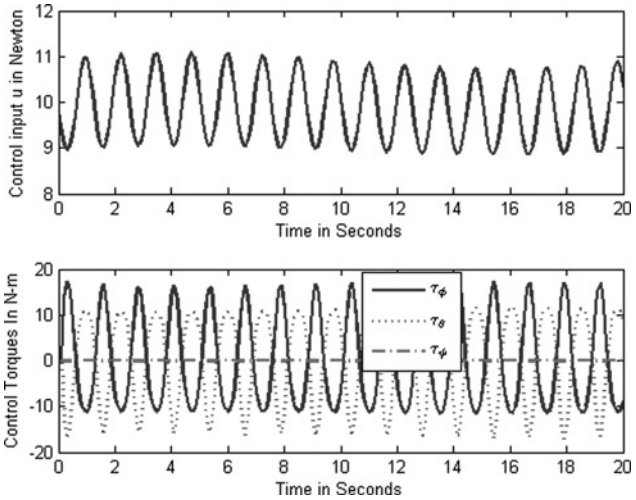

Figure 12 *Force and torque input variations (with input disturbances)*

doi: 10.1049/iet-cta:20080002

7 Conclusion

A two-loop approach using input–output linearisation to design a nonlinear controller for a quadrotor dynamics is discussed in this paper. Using this approach, an intuitively structured controller was derived that has an outer proportional derivative loop and an inner feedback linearising control loop. The dynamics of a quadrotor is a simplified form of helicopter dynamics that exhibits the basic problems including underactuation, strong coupling, multi-input/multi-output. The derived controller is capable of dealing with such problems simultaneously and satisfactorily. As the quadrotor model discussed in this paper is similar to a full-scale, unmanned helicopter model, the same control configuration derived for a quadrotor is also applicable for a helicopter model. The simulation results with and without input disturbances are shown above. Some aspects still remain untouched. The controller shows high sensitivity to state disturbances, which may be in the interest of future research.

8 Acknowledgments

This work was supported by NSF grant NSF ECCS-0801330 and ARO grant ARO W91NF-05-1-0314.

9 References

[1] KOO T.J., SASTRY S.: 'Output tracking control design of a helicopter model based on approximate linearization'. Proc. 37th Conf. Decision and Control (IEEE, Tampa, FL, 1998)

[2] GAVRILETS V., METTLER B., FERON E.: 'Dynamic model for a miniature aerobatic helicopter'. MIT-LIDS Report 2003, LIDS-P-2580

[3] STEVENS B.L., LEWIS F.L.: 'Aircraft control and simulation' (Wiley, New York, 2003)

[4] ALTUG E., OSTROWSKI J.P., MAHONY R.: 'Control of a quadrotor helicopter using visual feedback'. IEEE Int. Conf. Robotics and Automation, Washington, DC, , 2002

[5] BIJNENS B., CHU Q.P., VOORSLUIJS G.M., MULDER J.A.: 'Adaptive feedback linearization flight control for a helicopter UAV'. AIAA Guidance, Navigation, and Control Conf. and Exhibit, San Francisco, CA, , 2005

[6] MADANI T., BENALLEGUE A.: 'Backstepping control for a quadrotor helicopter'. Proc. 2006 IEEE/RSJ Int. Conf. Intelligent Robots and Systems, Bejing, China, 2006

[7] MISTLER V., BENALLEGUE A., M'SIRDI N.K.: 'Exact linearization and non-interacting control of a-4 rotors helicopter via dynamic feedback'. 10th IEEE Int. Workshop on Robot–Human Interactive Communication, Paris, 2001

[8] MOKHTARI A., BENALLEGUE A., ORLOV Y.: 'Exact linearization and sliding mode observer for a quadrotor unmanned aerial vehicle', *Int. J. Robot. Automat.*, 2006, **21**, (1), pp. 39–49

[9] CASTILLO P., LOZANO R., DZUL A.: 'Modelling and control of mini flying machines' (Springer, 2005)

[10] KANELLAKOPOULOS I., KOKOTOVIC P.V., MORSE A.S.: 'Systematic design of adaptive controllers for feedback linearizable systems', *IEEE Trans. Autom. Control*, 1991, **36**, pp. 1241–1253

[11] KHALIL H.K.: 'Nonlinear systems' (Macmillan, New York, 1992)

[12] SLOTINE J.-J., LI W.: 'Applied nonlinear control' (Prentice Hall, 1991)

[13] KIM B.S., CALISE A.J.: 'Nonlinear flight control using neural networks', *J. Guidance Control Dyn.*, 1997, **20**, (1), pp. 26–33

[14] PRASAD J.V.R., CALISE A.J.: 'Adaptive nonlinear controller synthesis and flight evaluation on an unmanned helicopter'. Proc. 1999 IEEE Int. Conf. Control Applications, Kohala Coast-Island of Hawaii, USA, 1999

[15] CALISE A.J., KIM B.S., LEITNER J., PRASAD J.V.R.: 'Helicopter adaptive flight control using neural networks'. Proc. 33rd Conf. Decision and Control, Lake Buena Vista, FL, , 1994

[16] HOVAKIMYAN N., NARDI F., CALISE A.J., LEE H.: 'Adaptive output feedback control of a class of nonlinear systems using neural networks', *Int. J. Control*, 2001, **74**, (12), pp. 1161–1169

[17] RYSDYK R., CALISE A.J.: 'Robust nonlinear adaptive flight control for consistent handling qualities', *IEEE Trans. Control Syst. Technol.*, 2005, **13**, (6), pp. 896–910

[18] WISE K.A., BRINKER J.S., CALISE A.J., ENNS D.F., ELGERSMA M.R., VOULGARIS P.: 'Direct adaptive reconfigurable flight control for a tailless advanced fighter aircraft', *Int. J. Robust Nonlinear Control*, 1999, **9**, (14), pp. 999–1012

[19] MCFARLAND M.B., CALISE A.J.: 'Nonlinear adaptive control of agile anti-air missiles using neural networks', *IEEE Trans. Control Syst. Technol.*, 2000, **8**, (5), pp. 749–756

[20] CAMPOS J., LEWIS F.L., SELMIC C.R.: 'Backlash compensation in discrete time nonlinear systems using dynamic

inversion by neural networks'. Proc. 2000 IEEE Int. Conf. Robotics and Automation, San Francisco, CA, , 2000

[21] CASTILLO P., LOZANO R., DZUL A.: 'Stabilization of a mini rotorcraft having four rotors', *IEEE Control Syst. Mag.*, 2005, **25**, (6), pp. 45–55

[22] BOUABDALLAH S., NOTH A.E., SIEGWART R.: 'PID vs LQ control techniques applied to an indoor micro quadrotor'. Int. Conf. Intelligent Robots and Systems (IEEE, Sendai, Japan, 2004), pp. 2451–2456

[23] LEWIS F., JAGANNATHAN S., YESILDIREK A.: 'Neural network control of robot manipulators and nonlinear systems' (Taylor & Francis, London, 1999)

[24] HOGAN N.: 'Adaptive control of mechanical impedance by coactivation of antagonist muscles', *IEEE Trans. Autom. Control*, 1984, **29**, pp. 681–690

[25] FLASH T., HOGAN N.: 'The coordination of arm movements: an experimentally confirmed mathematical model', *J. Neuro Sci.*, 1985, **5**, pp. 1688–1703

IET Control Theory Appl., 2009, Vol. 3, Iss. 3, pp. 303–314
doi: 10.1049/iet-cta:20080002